FE MODELING OF THIN-WALLED SMART STRUCTURES

Gil RAMA

Department of Structural Analysis, TU Berlin

Abstract

The concept of smart structures offers wide possibilities for improvements of transport structures. It enables safer and more robust designs with improved dynamics. An efficient 3-node shell element capable of modeling smart thin-walled structures is presented. The Mindlin-Reissner kinematics and equivalent single-layer approach are employed in the element formulation. The discrete shear gap (DSG) technique is used to eliminate the shear locking effects and strain smoothing technique to improve the performance. Piezoelectric layers are assumed to be polarized in the thickness direction. The electro-mechanical coupling between the in-plane strains and the electric field in the thickness direction is considered. The co-rotational FE formulation is used in order to take geometrically nonlinear effects into account. Numerical examples cover linear and geometrically nonlinear static and dynamic cases.

Key words: FEM, Shell, Nonlinear vibration simulation, Smart structures, Piezoelectric

1 INTRODUCTION

Fiber-reinforced thin walled composite are increasingly utilized in the designs of aerospace, naval and automotive applications and other transportation designs. Besides their high specific stiffness and strength they enable the integration of multi-functional materials e.g. piezo electric materials. Those materials create new design opportunities by changing the concept of structures from passive, load carrying systems to active/adaptive systems capable of sensing and actuating. The objectives are active vibration suppression, shape control, noise reduction (Fig. 1), health monitoring, etc. Piezoelectric materials are characterized by a sufficiently strong coupling between the mechanical and the electric fields, so that they can be employed as actuator as well as sensor devices which are widely utilized in the transportation industry. The continuous development of new complex structural designs and materials demands reliable and efficient numerical tools for modeling and simulation of the elastic behavior of those thin-walled structures. The Finite Element Method (FEM) has established itself as the method of choice for problems in the field of structural analysis. Shell type finite elements are usually addressed as numerically more efficient for the simulation of thin walled structures. The main requirements for shell elements are high efficiency, reliability and applicability over a wide range of thickness and curvature.

***Fig. 1** An example of a smart structure – car roof with active elements for noise reduction*

The requirement for high efficiency points to low-order elements. Most of the low order composite shell FE formulations are based on the equivalent single-layer approach and mainly rely on the Kirchhoff-Love or Mindlin-Reissner kinematics. Low order Mindlin-Reissner elements are notorious for shear locking effects for rather thin structures. The present element formulation utilized the discrete shear gap (DSG) technique proposed by Bletzinger [1] to alleviate the transverse shear locking effects.

Thin-walled structures are rather prone to geometrically nonlinear behavior, particularly due to significant local rotations and the developed FEM formulations need to account for this aspect. Regarding the coverage of geometric nonlinearities, the high efficiency request imposes the need to reconsider various formulations for description of nonlinear kinematics. Typical approach in commercially available software packages are the total and updated Lagrangian formulations, which offer rather high accuracy and reliability. The present formulation uses the co-rotational approach in order take geometrically nonlinear effects into account. The basic idea of the co-rotational approach is to separate the rigid-body motion from the total motion in order to obtain the purely deformational part.

The present work puts focus onto a highly efficient 3-node shell element for nonlinear static and dynamic analysis of smart thin-walled structures. Several cases are presented to demonstrate the applicability of developed element and formulation.

2 FEATURES OF THE PIEZOELECTRIC COMPOSITE SHELL ELEMENT

The present composite element is based on the equivalent single-layer approach and has five mechanical degrees of freedom, three translations and two rotations, per node and,

and as many electrical degrees of freedom as piezolayers. The electrical degrees of freedom are the electric potential differences of the piezolayers. The mechanical field is approximated by the Cell Smoothed – Discrete Shear Gap (CS-DSG) formulation. The Mindlin-Reissner kinematical assumptions are utilized in order to include transverse shear effects. The discrete shear gap technique suggested by Bletzinger [1] is implemented to eliminate the transverse shear locking effects. The strain smoothing technique proposed by Nguyen-Thoi et al. [2] is utilized to improve the accuracy and stability of the element. In addition the element formulation becomes independent of the node numbering sequence. Stress stiffening is taken into account by means of the geometric stiffness matrices $[K_\sigma]$.

One of the element main features is the piezoelectric coupling. The coupling is achieved by the e_{31}-effect, which implies that the in-plane strain field is coupled to the electric field acting in the thickness direction. Electric field E within the piezoelectric layers is assumed to be constant, which leads to a linear distribution of electric potential, φ, across the thickness so that the following relations hold:

$$E = -\frac{\partial \varphi}{\partial z'} \;\Rightarrow\; E_k = -\frac{\Phi_k}{h_k} \tag{1}$$

where Φ_k is the difference of electric potentials between the electrodes and h_k is the layer thickness (k in the subscript pertains to the layer number in the sequence of layers).

The mechanical strain and stress fields as well as the electro-mechanical coupling is developed in a local element coordinate system (x', y', z') presented in Fig. 2. Afterwards the elements matrices are transformed to the global coordinate system (x, y, z) and assembled to the corresponding system matrices. For a more detailed description of the element formulation see [3].

The element formulation is extended to the geometrically nonlinear analysis by means of the element-based co-rotational (CR) FE formulation. The implemented CR FEM formulation is based on an element-based co-rotational frame attached to the element which performs the same rigid-body motion as the element. This allows separating the total element motion into the rigid-body part and deformational motion which is subsequent used to compute the internal forces and moments.
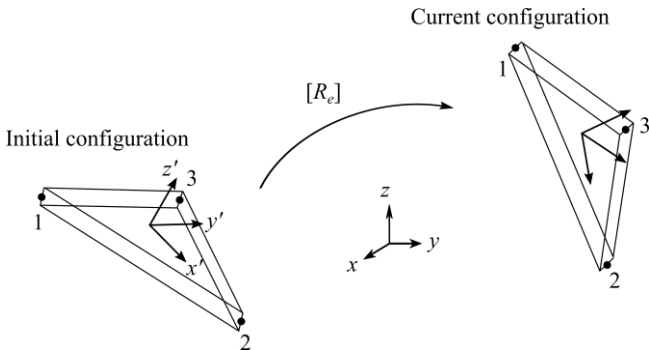
Fig. 2 *Total element motion as a superposition of rigid-body and deformational motion.*

The element stiffness matrix $[K_{uu,e}]$ is updated by means of rigid-body rotation matrix $[R_e]$. The deformational (rotation-free) displacements can then be determined by

$$\{F\} = {}^t[R_e][K_{uu,e}]\left({}^t[R]^{-1}\,{}^t\{x\} - {}^0\{x\}\right) \tag{2}$$

where $\{x\}$ is the element configuration (nodal coordinates) and the left superscript (t and 0) denote the moment in time at which the configuration is taken. The update of rotational degrees of freedom requires update of shell normals at each element node. This requires the incremental rotation matrix:

$$[Q] = [I] + \frac{\sin\gamma}{\gamma}[\tilde{s}] + \frac{1}{2}\left(\frac{\sin\frac{\gamma}{2}}{\frac{\gamma}{2}}\right)^2[\tilde{s}]^2 \tag{3}$$

where:

$$\gamma = \sqrt{\theta_1^2 + \theta_2^2 + \theta_3^2} \tag{4}$$

and the spin matrix:

$$[\tilde{s}] = \begin{bmatrix} 0 & -\theta_3 & \theta_2 \\ \theta_3 & 0 & -\theta_1 \\ -\theta_2 & \theta_1 & 0 \end{bmatrix} \tag{5}$$

with θ_1, θ_2 and θ_3 denoting the 3 incremental global rotations at the nodes. A more detail description of the co-rotational formulation can be found in [3].

3 FINITE ELEMENT EQUATIONS

The FE system of equations for a geometrically nonlinear dynamic analysis by means of an implicit time integration scheme reads:

$$\begin{aligned}
&\begin{bmatrix} [M_{uu}] & [0] \\ [0] & [0] \end{bmatrix} \begin{Bmatrix} {}^{t+\Delta t}\{\ddot{u}\}^{(k)} \\ \{0\} \end{Bmatrix} + \begin{bmatrix} {}^{t+\Delta t}[C_{uu}] & [0] \\ [0] & [0] \end{bmatrix} \begin{Bmatrix} {}^{t+\Delta t}\{\dot{u}\} \\ \{0\} \end{Bmatrix} \cdots \\
&+ \begin{bmatrix} {}^t[K_{uu}] + {}^t[K_\sigma] & {}^t[K_{u\phi}] \\ {}^t[K_{\phi u}] & {}^t[K_{\phi\phi}] \end{bmatrix} \begin{Bmatrix} {}^t\{\Delta u\}^{(k)} \\ {}^t\{\Delta\phi\}^{(k)} \end{Bmatrix} \cdots \\
&= \begin{Bmatrix} {}^{t+\Delta t}\{F_{ext}\} - {}^{t+\Delta t}\{F_{in}\}^{(k-1)} \\ {}^{t+\Delta t}\{Q_{ext}\} - {}^{t+\Delta t}\{Q_{in}\}^{(k-1)} \end{Bmatrix}
\end{aligned} \tag{6}$$

where $[M_{uu}]$ is the mass matrix, $[C_{uu}]$ the damping matrix, $[K_{uu}]$, $[K_\sigma]$, $[K_{u\phi}]$, $[K_{\phi u}]$ and $[K_{\phi\phi}]$ are mechanical stiffness, geometric stiffness, piezoelectric direct and inverse coupling, and dielectric stiffness matrices, respectively, while $\{\Delta\phi\}$, $\{\Delta u\}$, $\{\dot{u}\}$, $\{\ddot{u}\}$ are the incremental differences of electric potentials of the piezolayers, incremental displacements, nodal velocities and accelerations, respectively. On the right-hand side of the equations are external and internal forces and electric charges.

Piezoelectric layers could be employed as actuator or sensor. In the actuator case the piezo-layers are subjected to a predefined electric voltage, thus causing mechanical excitation due to the inverse piezoelectric effect. In the linear analysis the computation of induced mechanical loads ${}^t\{F_\phi\}$ is performed follows:

$${}^t\{F_\phi\} = [K_{u\phi}]\,{}^t\{\phi_a\} \tag{7}$$

In the nonlinear analysis the system matrices, including the piezoelectric coupling terms, have to be updated first. In the framework of the CR-formulation, the element piezoelectric coupling matrix is updated using element rotation matrix $^t[R_e]$:

$$^t[K_{u\phi}] = {}^t[R_e]\,{}^0[K_{u\phi}] \tag{8}$$

In the sensor case, the direct piezoelectric effect is used to induce electric voltage $^t\{\phi_s\}$ due to the external mechanical loads, whereby the external electric charges are equal to zero:

$$^t\{\phi_s\} = -[K_{\phi\phi}]^{-1}[K_{\phi u}]\,{}^t\{u\} \tag{9}$$

Rayleigh damping is used to introduce the dissipative effects in the FE equations. It consists of stiffness and mass proportional terms:

$$[C_{uu}] = \alpha[K_{uu}] + \beta[M_{uu}] \tag{10}$$

where α and β are the Rayleigh damping coefficients.

4   NUMERICAL EXAMPLES

In the following a set of examples is studied to demonstrate the applicability of the element for linear and geometrically nonlinear static and dynamic analysis. The examples include both nonlinear mechanical and electro-mechanical coupled cases (actuator, sensor and active damping cases).

4.1 Slit annular plate

The first case is an annular plate in the x-y plane with a slit. The inner radius of the plate is $R_i = 6$ m, the outer radius $R_o = 10$ m (Fig. 3). Plate thickness is t = 0.03 m. One side of the slit is clamped whereas the other side is subjected by two single forces F = 3 N acting in the z-direction in the points A and B that correspond to the outer and inner radius of the plate, respectively
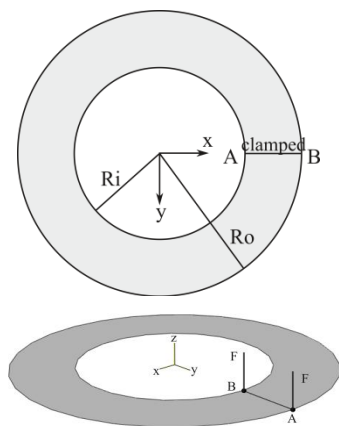

Fig. 3 *Slit annular plate: geometry in the x-y plane and loads.*

The Young's modulus is Y = $2.1 \cdot 10^7$ N/m^2, while the Poisson's coefficient 0. The initial and deformed configurations can be seen in Fig. 4, whereby the presented deformation is not scaled.
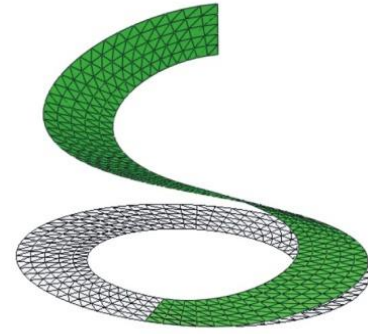

Fig. 4 *Original and deformed slit annular plate from two perspectives (without scaling).*

This case has been computed using the Abaqus S3 element and the current element formulation with a mesh consisting of 630 elements. The displacements of the point A are presented in Fig. 5. A very good agreement between the results from the presented element and formulation and from ABAQUS is obvious.
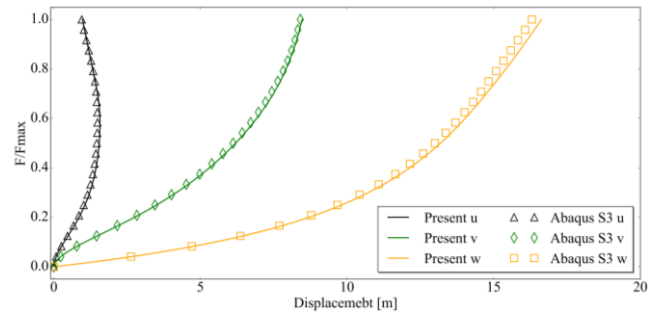

Fig. 5 *Slit annular plate Point A displacements.*

4.3 Piezoelectric Bimorph Beam

The piezoelectric bimorph beam consists of two uniaxial piezoelectric layers with opposite polarization. The geometry of the bimorph beam is shown in Fig. 6. The length L of the beam is 0.1 m, the height H is 0.1 mm and the width W is 5 mm. The beam made of uniaxial PVDF polarized in the thickness direction layers with following material properties: Y = 2.0 GPa, $\nu = 0.29$, $e_{31} = e_{32} = 0.046$ C/m^2 and $d_{31} = 0.1062 \cdot 10^{-9}$ F m^{-1}. In the following, the bimorph beam is considered as actuator and sensor in the linear analysis.
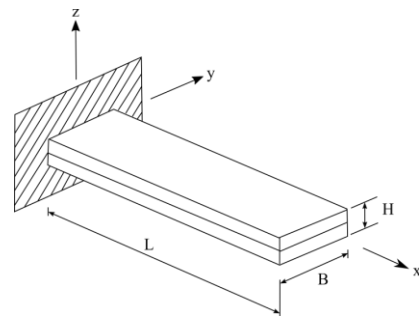

Fig. 6 *Bimorph beam geometry*

First the bimorph beam is considered as an actuator with a mesh of 40 elements. The beam is subjected by a voltage of $\Delta\varphi = 1$V. The obtained deflections are shown in Fig. 7. The

tip deflection obtained by the FE model using the present element is $3.45 \cdot 10^{-7}$ m which is also the analytically derived result based on the Euler-Bernoulli beam.

In the next case the beam acts as a sensor. A tip deflection of 0.01 m is imposed as a boundary condition. The expected step stair voltage distribution is verified by the obtained distribution of the electric voltage along the length of the beam for 6 and 20 sensors presented in Fig 8.
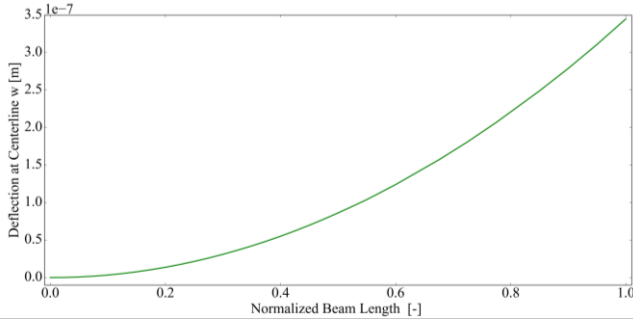

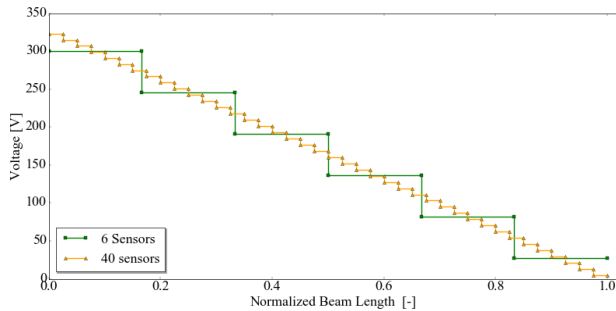***Fig. 7** Static deflection of bimorph beam subjected with input voltage of 1V*

***Fig. 8** Electric voltage distribution of the bimorph beam with an imposed tip deflection of 0.01 m*

4.4 Nonlinear dynamic analysis of a two-edge-simply-supported laminate

Fig. 9 depicts the geometry of a laminate composite plate simply supported over two shorter parallel edges. It consists of three layers – the 0.5 mm thick aluminum mid-layer and the 0.25 mm thick outer PTZ layers. The Young's modulus Y_{al} of the aluminum layer is 70.3 GPa and the Poisson's coefficient is 0.345. The PTZ layers are polarized in the thickness direction. Their material properties are: $Y_{11} = Y_{22} = 81.3$ GPa, $Y_{33} = 64.5$ GPa, $\nu_{12} = 0.29$, $\nu_{13} = \nu_{13} = 0.43$, $e_{31} = e_{32} = 14.8$ C/m^2 and $d_{31} = 1.15e \cdot 10^{-8}$ F m^{-1}.
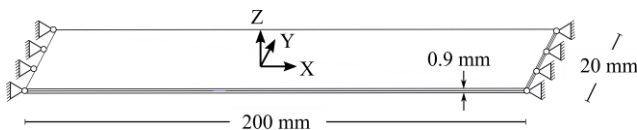

***Fig. 9** Geometry of the two-edge-simply-supported structure*

The structure subjected to time-variable electric voltage with amplitude of 100 V and frequency of 100 Hz. The response of the structure is observed in a time interval of 0.1 s. Newmark time integration scheme is employed with a time-step of 10^{-4} s. The structure's mid-point deflection is observed as a representative result. Linear and geometrically nonlinear dynamic responses are presented in Fig. 10. The geometrically nonlinear computation is verified by means of Abaqus. For the computation is Abaqus, the equivalent mechanical excitation is first pre-computed and then directly applied. It should be emphasized that the induced bending moments are of the follower type as their orientation depends on the current structural configuration. The appropriate option is used in Abaqus.
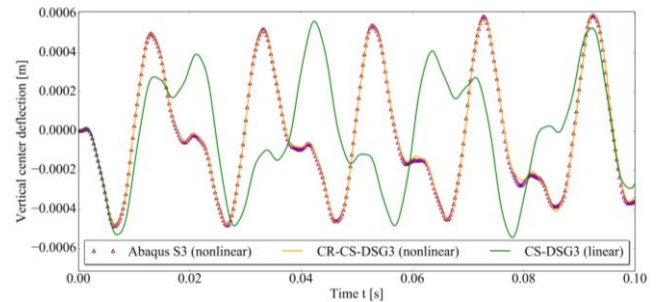

***Fig. 10** Two-edge-simply supported structure under harmonic excitation*

4.5 Vibration control of a simply supported piezoelectric plate (free vibration)

The next example illustrates the applicability of the present formulation in the active damping analysis using integrated sensors and actuators in the linear dynamic analysis.

Fig. 11 depicts the plate geometry together and the boundary conditions. The laminate consists of three layers - the outer two PTZ layers with the thickness of 0.1 mm and the steel mid-layer with the thickness of 0.5 mm. The steel material properties are: Young's modulus Y_{steel} is 210 GPa and the Poisson's coefficient is 0.30.
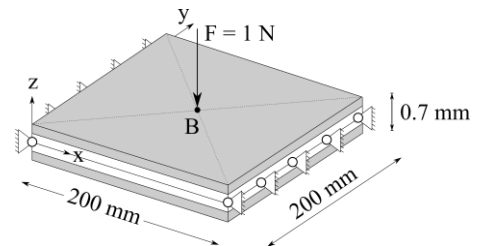

***Fig. 11** Simply supported piezoelectric plate geometry*

The isotropic PTZ layers are oppositely polarized in the thickness direction with following material properties: $Y_{PTZ} = 63.1$ GPa, $\nu = 0.3$, $e_{31} = e_{32} = 22.87$ C/m^2 and $d_{31} = 1.5e \cdot 10^{-8}$ F m^{-1}. The top layer is considered as a piezoelectric actuator labeled with subscript "a" and the bottom layer is a piezoelectric sensor denoted with subscript "s". The plate is discretized so that the FE mesh consists of 512 elements. When the structure oscillates, electric charges are induced in the sensor layer and converted into a velocity dependent voltage signal. This converted signal is then applied to the distributed actuator layer. As a result, resultant loads are generated to actively control the dynamic response of the structure. The resultant

active velocity feedback damping matrix $[C_{piezo}]$ can be expressed as:

$$[C_{piezo}] = G_v [K_{u\varphi}]_a [K_{\varphi\varphi}]_s^{-1} [K_{\varphi u}]_s \qquad (11)$$

where G_v is the dynamic feedback gain constant. The total structural damping matrix becomes:

$$[C] = [C_{uu}] + [C_{piezo}] \qquad (12)$$

The static configuration of the plate due to external force of F=1N was first determined. For the dynamic analysis, the force was removed and the structure starts to oscillate due to the pre-stressed state, i.e. internal forces. A damping ratio of 1.25 % is assumed. The linear transient response is solved by the Newmark integration method. The computations of the transient response are performed using a time step of 0.005s. Fig. 13 shows the time histories of the vertical center point B deflection with and without velocity feedback control (Gv = 0.0587). It can be seen that the induced piezo damping has a significant influence to the response of the structure.
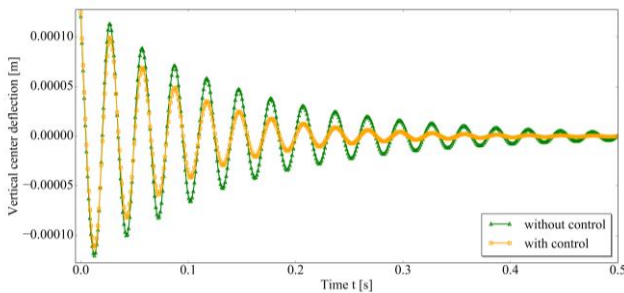
***Fig. 13** Transient response of the simply supported plate (free vibration) with and without velocity feedback control*

5 CONCLUSIONS

As a consequence of the optimization strategies of smart structures, an increased demand of effective numerical tools for their simulation is present. The presented element formulation provides an efficient tool for the computation of piezoelectric laminated structures involving fiber-reinforced composite layers. The element covers patches polarized in the thickness direction with the assumption of constant difference of electric potentials between the upper and lower surface of a piezoelectric patch.

Geometric nonlinearities are treated by means of CR-formulation, which is characterized by high efficiency and numerical stability.

The comparison with the commercially FEM software Abaqus demonstrated that the element provides highly accurate results for linear and geometrically nonlinear analysis.

The present class of active structures is a mere skeleton of what is perceived in the future. Their application is expected to be wider each day and spreading into new fields, including the field of transport characterized by pronounced dynamics. The developed numerical tools offer a solid basis for a successful design of adaptive/smart structures and their application in the field of transport in order to obtain solutions that would provide improved safety, comfort and longer life-time.

REFERENCES

1. Bletzinger, K.U., Bischoff, M., Ramm, E., 2000, *A unified approach for shear-locking-free triangular and rectangular shell finite elements*, Computers & Structures, 75(3), pp. 321-334.

2. Nguyen-Thoi, T, Phung-Van, P., Thai-Hoang, C., Nguyen-Xuan, H., 2013, *A Cell-based Smoothed Discrete Shear Gap method (CS-DSG3) using triangular elements for static and free vibration analyses of shell structures*, International Journal of Mechanical Sciences, 74, pp. 32-45.

3. Rama, G., Marinković, D., Zehn, M., 2017, *Efficient 3-node finite shell element for linear and geometrically nonlinear analysis of piezoelectric laminated structures*, Journal of Intelligent Material Systems and Structures, accepted for publishing.

Contact address:
Gil Rama,
Department of Structural Analysis, TU Berlin
10623 Berlin
Strasse des 17. Juni 135
E-mail: gil.rama@tu-berlin.de